Journal of Biomolecular NMR, 4 (1994) 463–482
ESCOM

J-Bio NMR 193

Determination of the NMR solution structure of the cyclophilin A–cyclosporin A complex

C. Spitzfaden[a,*], W. Braun[a], G. Wider[a], H. Widmer[b] and K. Wüthrich[a,**]

[a]*Institut für Molekularbiologie und Biophysik, Eidgenössische Technische Hochschule-Hönggerberg, CH-8093 Zürich, Switzerland*

[b]*Preclinical Research, Sandoz Pharma Ltd., CH-4002 Basel, Switzerland*

Received 18 January 1994
Accepted 18 February 1994

Keywords: Cyclosporin A; Cyclophilin; Immune suppression; NMR structure; Drug–receptor interaction

SUMMARY

The three-dimensional NMR solution structure of the cyclophilin A (Cyp)–cyclosporin A (CsA) complex was determined, and here we provide a detailed description of the analysis of the NMR data and the structure calculation. Using ^{15}N- and ^{13}C-resolved three- and four-dimensional [^1H,^1H]-nuclear Overhauser enhancement (NOE) spectroscopy with uniformly isotope-labeled Cyp in the complex, a final data set of 1810 intra-Cyp, 107 intra-CsA and 63 intermolecular NOE upper distance constraints was collected as input for the structure calculation with the program DIANA. A group of DIANA conformers, selected by a previously described analysis of the dependence of the maximal root-mean-square deviation (rmsd) among the individual conformers on the residual target function value, was subjected to energy refinement with the program FANTOM. The 22 best energy-refined conformers were then used to represent the solution structure. The average rmsd relative to the mean structure of these 22 conformers is 1.1 Å for the backbone atoms of all residues of the complex. The molecular architecture of Cyp in the Cyp–CsA complex includes an eight-stranded antiparallel β-barrel, which is closed on each side by an amphipathic helix. CsA is bound in a cavity formed by part of the barrel surface and four loops with nonregular secondary structure. Comparison of this structure with structures of Cyp–CsA and other Cyp–peptide complexes determined by different approaches shows extensive similarities.

INTRODUCTION

Cyclosporin A (CsA) is a member of a group of immunosuppressive drugs that bind with high affinity to their respective immunophilins (immunosuppressant-binding proteins) and act as inhibitors of specific signal transduction pathways that lead to T lymphocyte activation (Borel, 1986; Schreiber, 1991). The major receptor of CsA in T-cells is the cytosolic binding protein

*Present address: Department of Biochemistry, University of Oxford, Oxford OX1 3QU, U.K.
**To whom correspondence should be addressed.

cyclophilin A (Cyp) (Handschuhmacher et al., 1984), which is identical to the enzyme peptidyl-prolyl *cis-trans* isomerase (Fischer et al., 1989; Takahashi et al., 1989), of which CsA is a potent inhibitor. CsA is the favored therapeutic agent for prevention of graft rejection in clinical organ transplantation. In addition to the clinical importance of CsA, the fundamental interest in the molecular basis of immunosuppressive action has also spurred vigorous research activity on the Cyp–CsA system, which in recent years included structure determinations by NMR and by X-ray crystallography.

CsA is a cyclic undecapeptide with the sequence (Borel, 1986) c-[MeBmt-Abu-Sar-MeLeu-Val-MeLeu-Ala-D-Ala-MeLeu-MeLeu-MeVal], which contains the following unusual amino acids: MeBmt, (4*R*-4-[(*E*)-2-butenyl]-4,*N*-dimethyl-L-threonine; Abu, L-α-aminobutyric acid; Sar, sarcosine; MeLeu, *N*-methylleucine; MeVal, *N*-methylvaline. Cyclophilin A (Cyp) is the most abundant member of the family of cyclophilins. It is a water-soluble 165-residue protein with the amino acid sequence (Haendler et al., 1987):

```
          10                  20                  30                  40                  50
MVNPTVFFDI AVDGEPLGRV SFELFADKVP KTAENFRALS TGEKGFGYKG

          60                  70                  80                  90                 100
SCFHRIIPGF MCQGGDFTRH NGTGGKSIYG EKFEDENFIL KHTGPGILSM

         110                 120                 130                 140                 150
ANAGPNTNGS QFFICTAKTE WLDGKHVVFG KVKEGMNIVE AMERFGSRNG

         160
KTSKKITIAD CGQLE
```

A series of structural studies of the Cyp–CsA system was started with the determination of the conformation of Cyp-bound CsA (Fesik et al., 1991; Weber et al., 1991; Wüthrich et al., 1991a), which was found to be very different from those resulting from earlier structure determinations of free CsA in nonpolar solvents (Loosli et al., 1985). Subsequently, within less than two years, four different groups published about 10 structure determinations of free Cyp (Wüthrich et al., 1991b; Ke, 1992), Cyp complexed with a linear tetrapeptide as a model substrate for *cis-trans* isomerase activity (e.g. Kallen et al., 1991), and Cyp–CsA complexes (Spitzfaden et al., 1992b; Ke et al., 1993; Pflügl et al., 1993; Thériault et al., 1993). Simultaneously, additional structure determinations were performed with the functionally related system consisting of the immunosuppressant FK 506 and the FK 506-binding protein (e.g., Michnick et al., 1991; Moore et al., 1991). Our own work resulted first in the determination of the secondary structure of Cyp in solution (Wüthrich et al., 1991b), which was then used to support the tracing of a low-resolution electron density map to yield the crystal structure of a Cyp complex with a linear peptide (Kallen

---

Abbreviations: Cyp, cyclophilin A; CsA, cyclosporin A; NOE, nuclear Overhauser enhancement; NOESY, nuclear Overhauser enhancement spectroscopy; TOCSY, total correlation spectroscopy; 2D, 3D, 4D, two-, three-, four-dimensional; ct, constanttime; REDAC, redundant dihedral angle constraints; rmsd, root-mean-square deviation.

et al., 1991). Using this crystal structure of Cyp, the NMR structure of the bound CsA, and intermolecular NOE distance constraints identifying the Cyp–CsA contacts, a molecular model of the complex was generated (Spitzfaden et al., 1992a). Shortly thereafter we completed the NMR structure determination of the complex in solution (Spitzfaden et al., 1992b). The present paper describes the procedures used for this structure determination, and compares the results obtained with those reported by other groups.

MATERIALS AND METHODS

Sample preparation

Uniformly ^{15}N-labeled and [^{15}N,^{13}C]-doubly labeled human T-cell cyclophilin A was over-expressed in *E. coli*. Cells were grown on M9 minimal media containing either 1 g/l of [^{15}N]-ammonium sulphate as the sole nitrogen source, or 2 g/l of [^{15}N]-ammonium sulphate and 2 g/l of [$^{13}C_6$]-glucose as the sole nitrogen and carbon sources, respectively. The yield of purified protein obtained from this medium was 8 mg/l. ^{13}C-labeled CsA was a gift from Dr. R. Traber at Sandoz Pharma Ltd. The purification of Cyp and the preparation of NMR samples of the Cyp–CsA complex have been described previously (Weber et al., 1991).

NMR spectroscopy and collection of conformational constraints

NMR spectra of the Cyp–CsA complex were recorded on Bruker AMX spectrometers operating at proton frequencies of 500 or 600 MHz (T = 30 °C, pH = 6.0, complex concentration = 1.1 mM). The following heteronuclear 3D and 4D NMR experiments were used to extend the previously reported sequence-specific ^1H and ^{15}N assignments for the polypeptide backbone (Wüthrich et al., 1991b; Spitzfaden et al., 1992a) to the amino acid side-chain ^1H and ^{13}C resonances, and to collect NOE upper distance constraints as input for the structure calculation (Wüthrich, 1986): 3D ^{15}N-correlated [^1H,^1H]-NOESY (Fesik and Zuiderweg, 1988; Marion et al., 1989; Messerle et al., 1989) with uniformly ^{15}N-labeled Cyp bound to unlabeled CsA in 90% H_2O/10% D_2O, mixing time = 80 ms; 3D ^{13}C-correlated [^1H,^1H]-NOESY (Ikura et al., 1990; Zuiderweg et al., 1990) with ^{13}C-labeled Cyp bound to unlabeled CsA, solvent D_2O. Here, two different spectra were recorded with the ^{13}C carrier centered either in the aliphatic region at 38.8 ppm, or in the aromatic region at 136.5 ppm, with mixing times of 80 and 100 ms, respectively; 4D [^{13}C,^{13}C]-correlated [^1H,^1H]-NOESY (Clore et al., 1991; Zuiderweg et al., 1991) with ^{13}C-labeled Cyp bound to unlabeled CsA, solvent 90% H_2O/10% D_2O, mixing time = 100 ms; 2D [^1H,^1H]-NOESY with $^{13}C(\omega_1,\omega_2)$-double-half-filter (Otting and Wüthrich, 1990; Wider et al., 1990,1991) using ^{13}C-labeled CsA bound to unlabeled Cyp, solvent D_2O, only the $^{13}C(\omega_2)$-selected-$^{13}C(\omega_1)$-filtered subspectrum containing the intermolecular NOEs was used; 3D ^{13}C-correlated [^1H,^1H]-NOESY with ^{13}C-labeled CsA bound to unlabeled Cyp, solvent D_2O, mixing time 90 ms; 3D [HCCH]-TOCSY (Bax et al., 1990; Fesik et al., 1990) with ^{13}C-labeled Cyp bound to unlabeled CsA, solvent D_2O, TOCSY mixing time 21 ms; and 3D ct-[HCCH]-TOCSY with ^{13}C-labeled Cyp bound to unlabeled CsA, solvent D_2O, mixing time 7 ms. A constant-time scheme (Powers et al., 1991; Van de Ven and Philippens, 1992) was applied for simultaneous ^{13}C chemical shift labeling and ^{13}C-^1H coupling evolution, with a maximal evolution time in the ^{13}C time domain of $t_{1max} = 1/2\ {}^1J_{^{13}C^1H}$. The data were processed with the software package PROSA (Güntert et al., 1992). Prior to Fourier transformation, the time-domain data along the heteronuclear dimensions

were extended by linear prediction and zero-filling. The software package EASY was used for computer-supported spectral assignments (Eccles et al., 1991). NOESY cross-peak volumes in 3D spectra were determined using in-house written software, and translated into distance constraints with the program CALIBA (Güntert et al., 1991a).

Structure calculations

Preliminary structure calculations with the distance geometry program DIANA (Güntert et al., 1991a) were performed on a Cray Y-MP supercomputer. The final structure calculations were again performed using distance geometry in dihedral-angle space (Braun and Gō, 1985; Braun, 1987) with a version of DIANA that was optimized for parallel processing on an ALLIANT FX2800 computer (Widmer et al., 1993). For improved convergence, the REDAC procedure (redundant dihedral-angle constraints) was used (Güntert and Wüthrich, 1991). The covalent structures of the modified amino acids MeBmt, Abu, Sar, MeLeu and MeVal of CsA were generated with the program package GEOM (Sanner et al., 1989), and the standard DIANA library (Güntert et al., 1991a) was extended with the stereochemical data of these residues.

To perform structure calculations of the Cyp–CsA complex in dihedral-angle space, a covalent geometry of the randomized starting conformers was generated for the entire complex by the introduction of a linker peptide of 34 dummy glycyl residues with vanishing van der Waals radii linking the N-terminus of CsA and the C-terminus of Cyp. The calculations showed that the maximal length of the linker peptide, which corresponds to ca. 2.6 times the largest diameter of Cyp (ca. 40 Å), was sufficient for an unbiased sampling of all possible relative orientations of the ligand CsA and the receptor protein Cyp, although the C-terminus and the ligand binding site are on opposite faces of the Cyp molecule. Because the linker peptide is unrestrained, the ligand and the receptor will fold independently, until at higher target function levels intermolecular constraints are also considered. Due to the different sizes of the two components in the system under study, the folding of CsA will be completed at a target function level where Cyp is only partially folded. As a consequence, unfavorable interactions between the two components could prevent or slow down the folding of the receptor. However, in different strategies for the structure calculation, where intermolecular distance constraints were introduced either from the start of the DIANA calculations or only after the folding of the individual components was completed, no significant differences in the rate of convergence or in the quality of the resulting conformers were observed.

Selection of well-converged DIANA conformers and energy refinement

For the final selection of the DIANA conformers representing the solution structure, conformers were sorted according to their final DIANA target function values (Widmer et al., 1993). For a conformer with target function value TF, the pairwise backbone rmsd values for the well-defined regions of the complex were calculated relative to all conformers with lower target function values, and the maximum of these rmsd values ($rmsd_{max}$) was plotted as a function of TF. Horizontal plateau values of this plot indicate ranges of the target function values over which no additional conformational space is explored. These plateau values can be used as robust selection criteria for the best conformers, as has been shown in test calculations with the basic pancreatic trypsin inhibitor (Widmer et al., 1993). The DIANA conformers thus selected were subjected to energy refinement with the program FANTOM (Schaumann et al., 1991; Von Freyberg and

Braun, 1993). To ensure planarity of the peptide bonds, the torsion potential for ω-angles was increased fivefold relative to the ECEPP/2 potential (Némethy et al., 1983; Von Freyberg et al., 1993a) during the refinement. The standard minimization protocol (Von Freyberg et al., 1993b) was used. The results of the structure calculations were analyzed with the program XAM (Xia, 1992).

RESULTS AND DISCUSSION

Sequence-specific resonance assignments

We previously assigned the ^{1}H and ^{15}N polypeptide backbone resonances of CsA-bound Cyp (Wüthrich et al., 1991b; Spitzfaden et al., 1992a), and all ^{1}H and ^{13}C resonances of Cyp-bound CsA (Weber et al., 1991). These earlier data were now confirmed and complemented by assignments for the ^{1}H and ^{13}C resonances of the amino acid side chains of Cyp using 3D [HCCH]-TOCSY with a mixing time of 21 ms, 3D ct-[HCCH]-TOCSY with a mixing time of 7 ms, 3D ^{13}C-correlated [^{1}H,^{1}H]-NOESY, 3D ^{15}N-correlated [^{1}H,^{1}H]-NOESY and 4D [^{13}C,^{13}C]-correlated [^{1}H,^{1}H]-NOESY.

The $^{13}C^{\alpha}$ chemical shifts of Cyp were assigned, based on the observation of similar NOESY

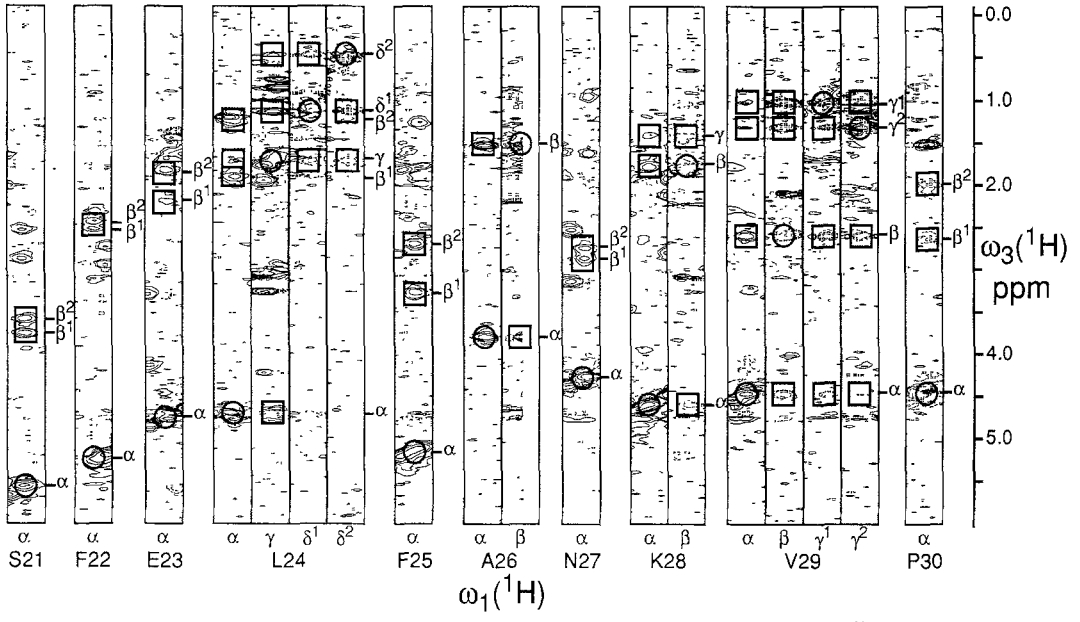

Fig. 1. Illustration of the amino acid side-chain resonance assignments for the segment Ser^{21}–Pro^{30} of the Cyp polypeptide chain. For each residue, selected regions (strips) from $\omega_1(^1H)$–$\omega_3(^1H)$-planes of a 3D ct-[HCCH]-TOCSY spectrum, recorded with a mixing time of 7 ms (see Table 1), of a complex between uniformly [^{13}C,^{15}N]-doubly labeled Cyp and unlabeled CsA are shown. Strips along $\omega_3(^1H)$ with a width of 0.2 ppm in the $\omega_1(^1H)$-dimension were taken at the ^{13}C frequencies of the (^{1}H,^{13}C)-direct correlation peaks ($\omega_1 = \omega_3$, indicated by circles). The individual strips are identified by the atom positions on the right, and the spin-system assignments at the bottom (the strip for Ala^{26} β was at the edge of the spectral width along ω_1, and therefore the right half of the signal is truncated). TOCSY cross peaks along the ω_3 dimension are indicated by boxes and assignments are given on the right side of the presentation for each residue. Dashed lines indicate negative signal intensities of folded peaks.

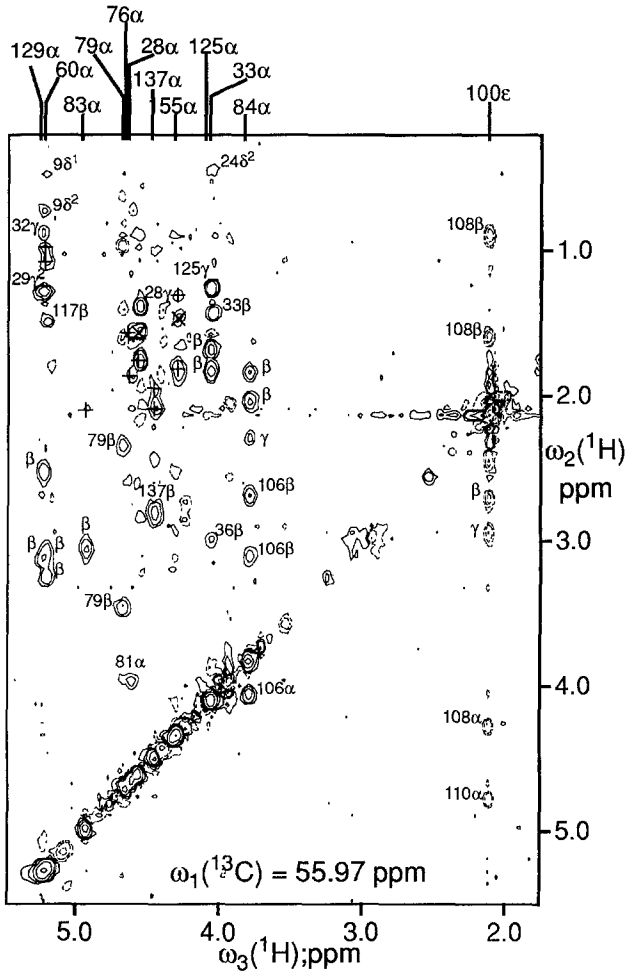

Fig. 2. Region (ω_2(^{1}H) = 0.2–5.3 ppm, ω_3(^{1}H) = 1.8–5.3 ppm) of the [^{1}H,^{1}H]-plane at ω_1(^{13}C) = 55.97 ppm from a 3D ^{13}C-correlated [^{1}H,^{1}H]-NOESY spectrum of a complex between uniformly [^{13}C,^{15}N]-doubly labeled Cyp and unlabeled CsA. The selected area contains all the signals in this particular [^{1}H,^{1}H]-plane. The assignments of the direct 'diagonal' correlation peaks ($\omega_2 = \omega_3$) present in this plane are given at the top of the spectrum by the residue number and the atom position. Some cross peaks are labeled in the spectrum; for intramolecular cross peaks only the atom positions are given, for intermolecular cross peaks also the residue number. In cases of degenerate C$^\alpha$H frequencies along ω_2, the labels are positioned on the same side of the cross peaks as the assignment at the top. In crowded regions, + and × indicate assigned and unassigned cross peaks, respectively. Dashed contour lines indicate negative intensity levels of folded peaks.

patterns of the amide and C$^\alpha$ protons of a given spin system in the ^{15}N- and ^{13}C-correlated NOESY spectra, where the exact C$^\alpha$ frequencies were taken from a [^{13}C,^{1}H]-COSY spectrum recorded with a digital resolution along the ^{13}C axis of 0.1 ppm. The C$^\alpha$ resonance assignments are complete, except for Gly^{64}, Gly^{65}, Gly^{75} and Gln^{111}. The C$^\alpha$ chemical shifts thus obtained agree within ± 0.5 ppm with those reported from assignments based on coherent magnetization transfer using triple-resonance experiments (Neri et al., 1991), with the exception of Pro^4 ($\Delta\delta$ = 5.8 ppm), Asp^{13} ($\Delta\delta$ = 1.1 ppm), Ser^{51} ($\Delta\delta$ = 0.6 ppm) and Cys^{52} ($\Delta\delta$ = 0.9 ppm).

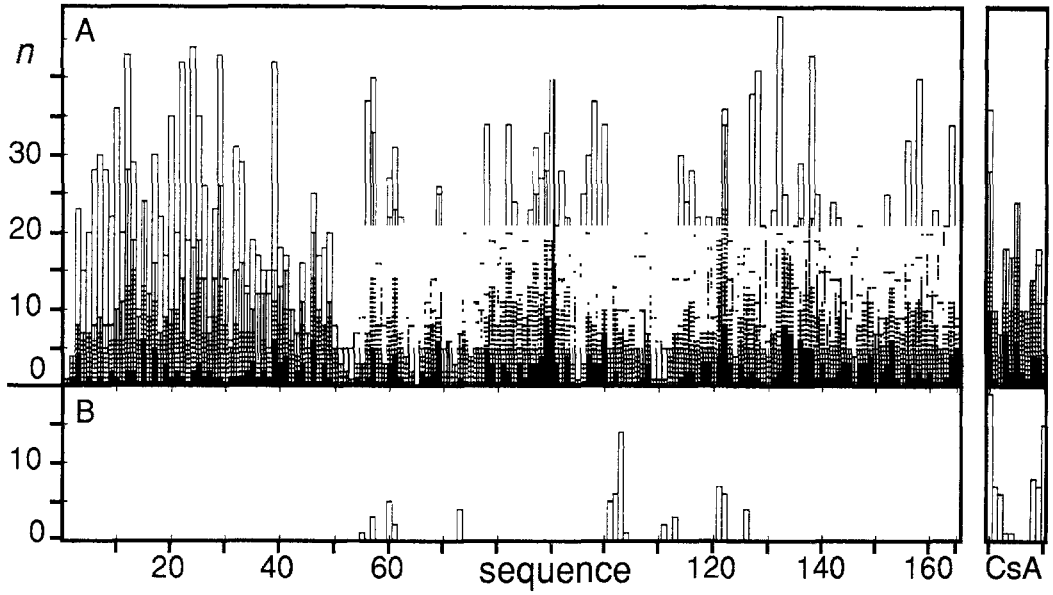

Fig. 3. (A) Plot of the number and types of intramolecular NOE-derived upper distance constraints per residue versus the amino acid sequences of Cyp and CsA, used for the structure calculation of the Cyp–CsA complex in solution. The following code was used to define the different classes of NOE constraints (Wüthrich, 1986): black, intraresidual (304); cross-hatched, sequential (187); vertically hatched, medium- and long-range backbone (240); empty, long-range involving side chains (1079). (B) Sequence distribution of the 63 intermolecular NOE upper distance constraints.

Figure 1 shows the spectral analysis of the 3D ct-[HCCH]-TOCSY data for the polypeptide segment Ser^{21}–Pro^{30}. The intervals for the refocusing and defocusing of ^{13}C magnetization were optimized for preferential magnetization transfer from methine to methylene groups (i.e., $C^{\alpha} \rightarrow C^{\beta}$), to avoid loss of signal due to compromised refocusing delays. The resulting spectrum was asymmetric with respect to the cross-peak intensities on the two sides of the diagonal, and for many spin systems one of the two symmetry-related correlation peaks corresponding to the transfer $C^{\beta} \rightarrow C^{\alpha}$ was very weak or even absent (for example, those spin systems in Fig. 1 for which only one strip is shown, that is, Ser^{21}, Phe^{22}, Glu^{23}, Phe^{25}, Asn^{27} and Pro^{30}). In these cases, 3D and 4D ^{13}C-correlated NOESY spectra were used in addition to 3D [HCCH]-TOCSY to identify the symmetry-related cross peaks and to determine the $^{13}C^{\beta}$ resonance frequencies. With the signal-to-noise ratio obtained (Fig. 1), the 3D [HCCH]-TOCSY spectra yielded the desired assignments for the spin systems of the AMX type and for those bearing methyl groups, whereas for other residues with long side chains only few assignments were obtained for methylene groups beyond the β-position. With the resulting incomplete set of sequence-specific ^{1}H and ^{13}C resonance assignments we started a first round of peak assignments in the 3D and 4D ^{13}C-correlated NOESY spectra, and initial structure calculations were performed using the input thus obtained.

Assignments for the peripheral parts of residues with long side chains and for the aromatic side chains were then extracted from the 3D and 4D ^{13}C-correlated and 3D ^{15}N-correlated NOESY spectra, in conjunction with further rounds of collection of conformational constraints. Thereby, NOESY cross peaks were assigned as intraresidual NOEs to peripheral hydrogen atoms in long side chains, if the connected ^{13}C resonance frequencies were within the characteristic ranges

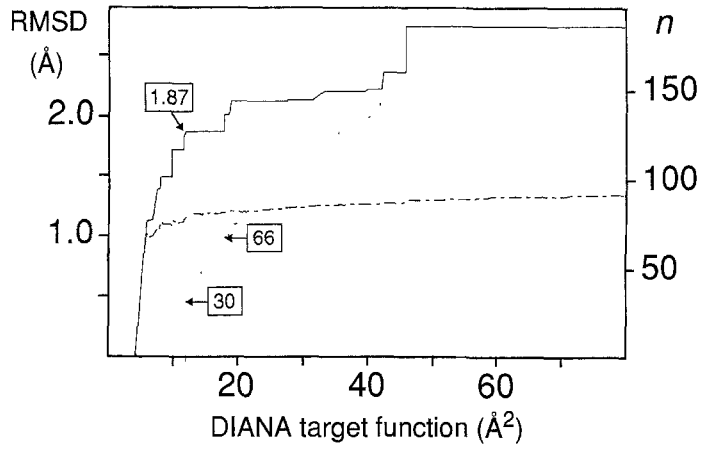

Fig. 4. Selection of a group of 'best' DIANA conformers of the Cyp–CsA complex. Of the 200 conformers, 180 (n on the right) had residual target function values ≤ 80 Å (plotted along the horizontal axis). The conformers were arranged according to the residual DIANA target function value, and the dotted line represents the number of conformers with target functions below the value on the horizontal axis. For each conformer the maximal pairwise rmsd, $rmsd_{max}$, relative to all conformers with smaller target functions is plotted (solid line), and the dash-dotted line represents the average of all these pairwise rmsd values. Rmsd values were calculated for the backbone atoms N, C^{α} and C' of residues 3–39, 53–63, 91–102, 111–118, 129–143 and 154–164 of Cyp and all residues of CsA, which were found to be well defined after a preliminary analysis of the DIANA conformers.

expected for the amino acid types as determined by the sequence-specific assignments of the backbone resonances, and if all proton–proton distances derived from these intraresidual NOE assignments were consistent with the primary, secondary and eventually tertiary structures.

A list of those ^{1}H, ^{13}C and ^{15}N resonance assignments which resulted exclusively from scalar connectivities was submitted to the Brookhaven Protein Data Bank, together with the atom coordinates of the NMR solution structure (entry code 3CYS). The following is a brief summary of the assignments obtained: (i) The assignments for the 23 glycine residues are complete, except for H^{α} of Gly^{65} and $^{13}C^{\alpha}$ of glycines 64, 65 and 75. (ii) For the nine alanines, 11 threonines and nine valines, complete ^{1}H assignments were obtained from scalar coupling connectivities. The same holds for the seven leucines and 10 isoleucines, except that for the assignment of some of the methylene groups we had to rely on 3D ^{13}C-correlated NOESY, and that the $C^{\gamma}H_2$ group of Ile^{56} was not assigned. Only a small number of ^{13}C chemical shifts could not be determined in this group of residues. For the diastereotopic pairs of methyl groups of valine and leucine, stereospecific assignments were obtained by biosynthetically directed fractional ^{13}C labeling (Neri et al., 1989). (iii) For the 50 AMX spin systems of the $C^{\alpha}H$-$C^{\beta}H_2$ fragments of eight serines, four cysteines, seven aspartic acids, nine asparagines, four histidines, 15 phenylalanines, two tyrosines and one tryptophan (Ser^{21}, Phe^{22}, Phe^{25} and Asn^{27} are shown in Fig. 1), complete ^{1}H assignments were obtained from scalar coupling connectivities, except for Cys^{52}, Phe^{53} and His^{54}, which had weak signal intensities and for which partial assignments resulted from NOEs. For most AMX spin systems, only the $C^{\alpha} \rightarrow C^{\beta}$ magnetization transfer was observed in the specially tuned ct-[HCCH]-TOCSY experiment (see Fig. 1). For the identification of the symmetry-related $C^{\beta} \rightarrow C^{\alpha}$ connectivities, which are necessary for the assignment of the C^{β} resonances, we resorted in

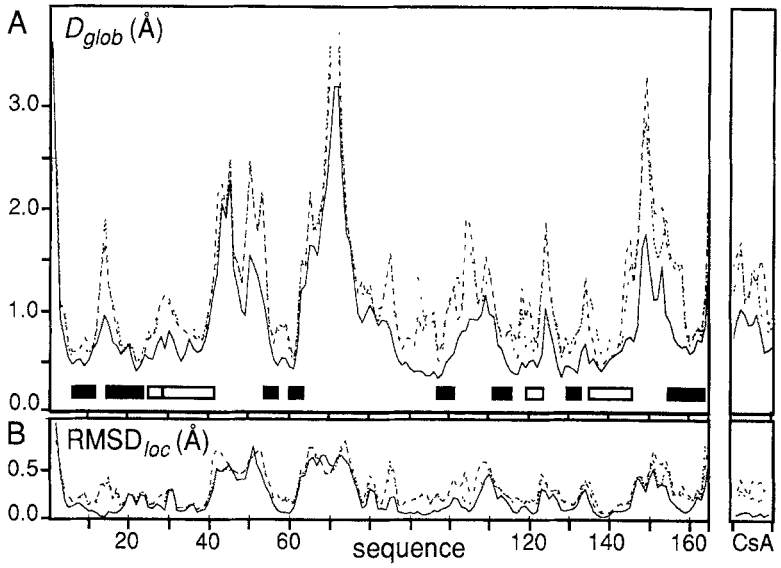

Fig. 5. Comparison of the local backbone conformations of the NMR solution structure, the X-ray crystal structure (Pflügl et al., 1993) and the previously reported molecular model (Spitzfaden et al., 1992a) of the Cyp–CsA complex. (A) Plots against the amino acid sequence of the average global backbone displacement (D_{glob}) (Billeter et al., 1989) relative to the mean NMR structure (solid line) for the individual amino acid residues of the 22 energy-minimized conformers after superposition of the backbone atoms N, C^{α} and C' in the well-ordered segments 3–65 and 76–164 of Cyp and all residues of CsA. The rmsd values relative to the crystal structure (dotted line), and relative to the molecular model of Spitzfaden et al. (1992a) (dashed line) are also given. (B) Local backbone rmsd relative to the mean NMR coordinates (solid line) ($rmsd_{loc}$), calculated for all continuous tripeptide segments along the sequence and plotted for the central residues. The rmsd values relative to the crystal structure (dotted line) and the model (dashed line) are also shown. Horizontal bars indicate regions of regular secondary structure: black bars, β-sheets; open bars, α- or 3_{10}-helices.

most cases to the 3D ^{13}C-correlated NOESY spectrum. In addition to the ^{1}H and ^{13}C resonance frequencies, assignments were also obtained for the δNH_2 groups of the asparagine residues 2, 87, 102, 108 and 137, using the 3D ^{15}N-correlated NOESY spectrum. (iv) For the long side chains of 12 glutamic acids, three glutamines, five methionines, six prolines, six arginines and 14 lysines (Glu^{23}, Lys^{28} and Pro^{30} in Fig. 1), the β-methylene protons were assigned from scalar coupling connectivities in all cases, except Arg^{37}, Gln^{111}, Met^{136} and Arg^{144}. Scalar coupling connectivities to the γ-methylene protons were established for the majority of the glutamic acid, glutamine and methionine residues. Using NOE connectivities, complete ^{1}H assignments were obtained for all six prolines, Met^{100} and Met^{136}, and for all glutamic acid and glutamine residues except Glu^{23}, Glu^{34}, Gln^{63} and Gln^{111}; for the remaining residues partial spin system assignments were obtained with the use of NOESY. (v) Cyp contains 22 aromatic spin systems of 15 phenylalanines, two tyrosines, four histidines and one tryptophan, which gave rise to about 50 cross peaks in a 2D [^{13}C,^{1}H]-COSY spectrum. Further spectral analysis of the aromatic region was so far limited by the poor sensitivity due to the short ^{13}C transverse relaxation times, and probably by the fact that complete exchange of the amide protons in D_2O solution of Cyp had never been achieved (Wüthrich et al., 1991b). A 3D ^{13}C-correlated [^{1}H,^{1}H]-NOESY spectrum recorded with the ^{13}C carrier frequency in the aromatic region provided most of the information, in particular connec-

tivities between the aromatic rings and $C^{\beta}H_2$ (Wüthrich, 1986). Eventually, using exclusively NOE connectivities, complete assignments were obtained for the aromatic rings of the phenylalanine residues 22, 46, 60 and 83, Tyr^{79} and Trp^{121}, and partial assignments for numerous additional aromatic rings and the four histidines.

The ^1H chemical shifts for Trp^{121} obtained in the present study coincide within ± 0.05 ppm with those published by Fesik et al. (1992). Chemical shifts for the other side chains have not been reported either for free Cyp or the Cyp–CsA complex.

Collection of input for the structure calculation

Intramolecular NOE upper distance constraints for Cyp were obtained primarily from the 3D heteronuclear ^{15}N- and ^{13}C-correlated [^1H,^1H]-NOESY spectra. An initial structure was calculated with 359 intramolecular medium- and long-range distance constraints (Spitzfaden et al., 1992b). These data were supplemented with constraints for 33 hydrogen bonds (Williamson et al., 1985) and 153 backbone dihedral angles; the latter constrained the residues in regular α-helical or β-sheet secondary structures to account for the previously identified regular secondary structures of Cyp (Wüthrich et al., 1991b). This initial set of intramolecular distance constraints for Cyp was expanded and the calibration parameters refined in iterative cycles of spectral analysis and structure calculation, which also resulted in more complete sequence-specific ^1H NMR assign-

TABLE 1
ANALYSIS OF THE 37 DIANA CONFORMERS SELECTED WITH THE PROCEDURE OF FIG. 4 BEFORE AND AFTER ENERGY MINIMIZATION WITH THE PROGRAM FANTOM[a]

Quantity	Average and standard deviation (range)	
	DIANA	DIANA + FANTOM
DIANA target function (Å^2)[b]	10.2 ± 2.9 (4.2–17.5)	
FANTOM energy (kcal/mol)[c]	3031 ± 452 (2365–4185)	6 ± 133 (−297–346)
Hydrogen-bond energy (kcal/mol)	18 ± 100 (−116–286)	−192 ± 9 (−210–−175)
Lennard-Jones potential (kcal/mol)	2003 ± 390 (1412–2840)	−378 ± 73 (−523–−226)
Torsion-angle energy (kcal/mol)	370 ± 16 (332–400)	305 ± 35 (234–384)
Residual distance constraint violations:		
Sum (Å)	20.1 ± 4.0 (11.1–29.3)	41.4 ± 3.0 (34.3–45.8)
Maximum (Å)	0.6 ± 0.2 (0.2–1.0)	0.43 ± 0.07 (0.30–0.56)
Residual dihedral-angle constraint violations:		
Sum (deg)	40.8 ± 11.0 (22.3–72.4)	152 ± 27 (112–226)
Maximum (deg)	9.2 ± 2.2 (6.2–15.1)	23.7 ± 2.5 (20.8–31.5)

[a] A total of 200 DIANA conformers were calculated, but only 37 selected conformers were subjected to energy minimization (see text).

[b] Relative weighting factors used during the DIANA calculations were 1 for NOE constraints, 2 for van der Waals lower limits, and 5 for dihedral-angle constraints. The target function is not defined after energy minimization, because the planarity of the peptide bonds is not strictly preserved.

[c] Total conformational energy (i.e., sum of the electrostatic, hydrogen-bonding, Lennard-Jones and torsion-angle potentials).

TABLE 2
QUANTITATIVE CHARACTERIZATION OF THE SOLUTION STRUCTURE OF THE Cyp–CsA COMPLEX AND COMPARISON WITH TWO OTHER MODELS[a]

Atoms used for the comparison	RMSD (Å)		
	NMR-<NMR>[b]	NMR-crystal[b]	NMR-model[b]
All residues of Cyp and CsA	1.10 (1.67)	1.48 (2.29)	1.52 (2.35)
Well-defined segments of Cyp and CsA[c]	0.68 (1.24)	1.02 (1.83)	1.01 (1.83)
CsA	0.20 (0.53)	0.48 (0.91)	0.72 (1.20)
Binding-site residues of Cyp and CsA[d]	0.74 (1.16)	0.94 (1.61)	0.96 (1.60)

[a] Our solution structure is compared to the X-ray structure of Pflügl et al. (1993) and to the model of Spitzfaden et al. (1992).

[b] NMR stands for the individual conformers; <NMR> is the mean of the 22 energy-refined conformers representing the solution structure; 'crystal' stands for the X-ray structure of Pflügl et al. (1993); 'model' stands for a molecular model of the complex derived from combined X-ray and NMR data (Spitzfaden et al., 1992). The numbers given are the average of the pairwise rmsd values for all 22 conformers relative to the mean structure, the X-ray structure and the model structure. For each entry the first number was calculated for the backbone atoms N, C^{α} and C', and the number in parentheses for all heavy atoms of the indicated backbone segments. The mean structure, <NMR>, was calculated in the following manner: The backbone atoms N, C^{α} and C' of the given peptide segments of conformers 2–22 were superimposed for minimal pairwise rmsd with the corresponding atoms of conformer 1, and the mean was calculated.

[c] Residues 3–39, 53–63, 91–102, 111–118, 129–143 and 154–164 of Cyp and 1–11 of CsA (these are the same residues as those used in the analysis of Fig. 4).

[d] The backbone atoms of all Cyp and CsA residues with intermolecular heavy-atom contacts of less than 7.0 Å and with a standard deviation of less than 1 Å among the 22 structures were considered, i.e., residues 55, 57, 59–61, 73, 100–104, 107–109, 111–113, 119, 121, 122 and 126 of Cyp, and residues 1–5 and 8–11 of CsA.

ments (see the preceding section). As an illustration of the quality of the NOE data used, Fig. 2 shows a [^{1}H,^{1}H]-cross plane from a 3D ^{13}C-correlated [^{1}H,^{1}H]-NOESY spectrum.

For CsA the previously used intra-CsA NOE upper distance constraints (Weber et al., 1991) were supplemented with seven NOE distance constraints from a 2D ^{13}C-correlated NOESY spectrum with a $^{13}C(\omega_1,\omega_2)$ double-half-filter (Wider et al., 1991) recorded in water. All these constraints involved the γ-hydroxyl proton of the MeBmt[1] side chain. In addition, the previously measured four $^3J_{HN\alpha}$ coupling constants for Cyp-bound CsA (Weber et al., 1991) were also used in the input.

All in all, 2747 intra- and intermolecular NOEs were assigned. Distance constraints involving $C^{\delta}H$ and $C^{\varepsilon}H$ of phenylalanine and tyrosine rings were in all cases referred to C^{γ} and C^{ζ} as 'pseudoatoms' (Wüthrich et al., 1983; Wüthrich, 1986). After pretreatment with the DIANA program (Güntert et al., 1991a,b) and excluding NOEs between protons with fixed distances, 1980 meaningful NOE upper distance constraints were derived, i.e., 1810 intra-Cyp, 107 intra-CsA and 63 intermolecular constraints. The distance constraints are quite evenly distributed over the entire sequence, except that less than 10 constraints per residue were found for the segments 43–45, 50–54, 70–72 and 109–111 (Fig. 3).

Structure calculation and selection of a representative group of 'best DIANA conformers'

The inclusion of backbone–backbone hydrogen-bond constraints and dihedral-angle con-

A

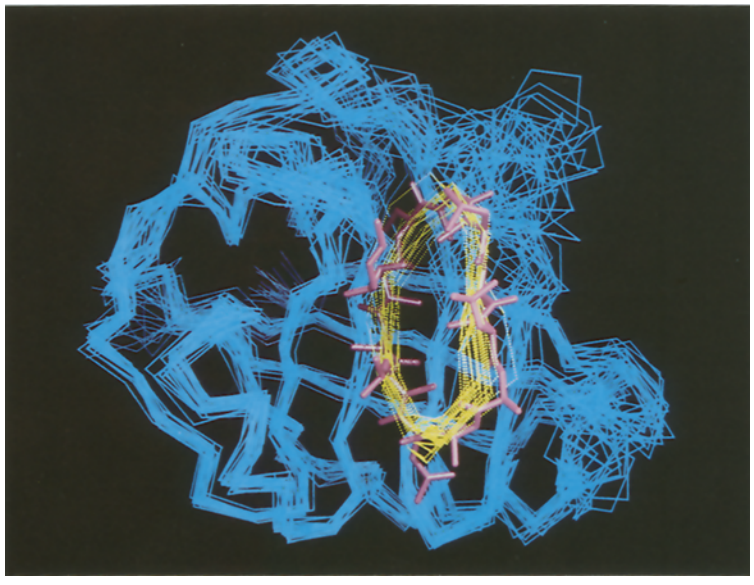

B

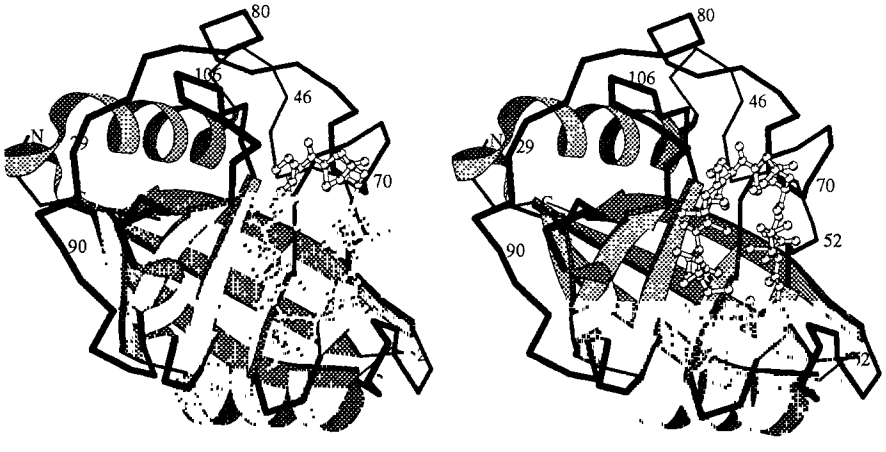

C

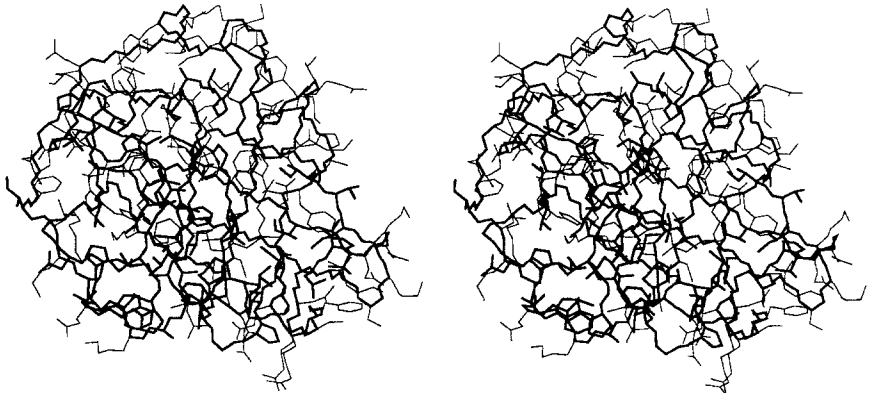

straints for residues in regular secondary structures, which had been used in the calculations of preliminary structures to represent previously identified secondary structure elements (Wüthrich et al., 1991b), was found not to be critical with regard to either the convergence of the structure calculations or the quality of the NMR structure when used in conjunction with the final input of NOE constraints. Thus, sets of conformers calculated either with or without these supplementary constraints were, after energy minimization, virtually indistinguishable, and the secondary structure hydrogen bonds were equally well defined in both sets of conformers. Therefore, these supplementary constraints were not included in the input for the final DIANA calculation, which was started with 200 randomized conformations. The REDAC procedure (Güntert and Wüthrich, 1991) was applied four times, followed each time by a DIANA computation at full target level, using only the experimental conformational constraints. Additional REDAC cycles did not significantly improve convergence. Although the final set of conformers did not contain any consistent constraint violations that would have occurred in a significant fraction of the conformers, the residual DIANA target function values within the group of 200 conformers were relatively high, with a mean value of 36 ± 32 Å^2 and a range from 4.2 to 188 Å^2.

To minimize possible bias of the DIANA target function in the selection of the group of 'best' conformers to be used to represent the solution structure, for example by factors such as the calibration of the NOE intensities or the conformational sampling properties, the criterion of 'similarity' indicated by common rmsd values in subgroups of conformers was applied as an additional selection criterion (Widmer et al., 1993). After sorting the DIANA conformers according to the residual DIANA target function values, $rmsd_{max}$ for each conformer (see the Materials and Methods section) was plotted versus the residual target function (Fig. 4). A strong dependence of $rmsd_{max}$ on the target function is observed for the 30 conformers with the lowest residual target function values. For target function values ≥ 12 Å^2, the plot contains extended plateaus, separated by distinct steps in the $rmsd_{max}$ values. On each plateau the same conformation space is covered by each conformer. For the selection of the 'best' structures we used the 66 conformers with $rmsd_{max} \leq 1.87$ Å. All 30 conformers with $rmsd_{max} < 1.87$ Å were included in this group, and of the 36 conformers with $rmsd_{max} = 1.87$ Å, every fifth conformer was selected. These 37 conformers represent one third of the total sample of 200 conformers, and satisfy the experimental distance constraints with a maximum residual violation of 0.6 ± 0.2 Å (Table 1). Due to the larger sample of 200 starting conformers, we had to increase the number of selected conformers

---

←

Fig. 6. (A) C^{α} plot of the polypeptide backbone of the 22 selected conformers representing the NMR solution structure of the Cyp–CsA complex (blue, Cyp; yellow, CsA; magenta: all-heavy-atom molecular model of CsA in the conformer with the lowest residual Lennard-Jones potential. The backbone atoms N, C^{α} and C' of the well-ordered regions of the 22 energy-refined DIANA conformers, i.e., residues 3–65 and 76–164 of Cyp and all residues of CsA, were superimposed for minimal rmsd. (B) Ribbon plot of the NMR structure of Cyp in the Cyp–CsA complex in the same orientation as in (A). The conformer with the lowest residual Lennard-Jones potential is shown. Elements of regular secondary structure are indicated as arrows (β-sheet) and ribbons (α- or 3_{10}-helix). Selected positions are identified with the sequence locations. CsA is shown as an all-heavy-atom molecular model in the same presentation as in (A). (C) All-heavy-atom representation of the conformer in (B) in a similar orientation. Heavy lines indicate the backbone heavy atoms and the 59 best defined side chains (residues 4–6, 10–12, 16, 17, 20–22, 26, 29, 30, 32, 33, 38, 39, 56–58, 60, 61, 89, 92, 93, 95, 97–99, 101, 103, 114–117, 119, 121–123, 127, 128, 132, 136, 138, 139, 141, 142, 156–159 and 164 of Cyp, and 1, 2, 5, 8, 10 and 11 of CsA), thin lines all other side chains. The drawings were prepared with the programs MidasPlus (Ferrin et al., 1988) and MolScript (Kraulis, 1991).

compared to the 'conventional' selection of the 20 conformers with the lowest target function (Güntert et al., 1991b). Figure 4 shows that the presently used selection criteria are quite robust with respect to the parameters used. As we will see below, in the case of the Cyp–CsA complex the final selection of conformers obtained with this procedure differs only little from what would have been obtained with the 'conventional' selection of about 20 DIANA conformers with the lowest residual target function values (Güntert et al., 1991b).

Energy refinement and final selection of conformers to represent the solution structure

Energy minimization with the program FANTOM reduced the mean energy of the aforementioned 37 DIANA conformers by about 3000 kcal/mol, with only a small increase of the sums of constraint violations (Table 1). Twenty-two energy-refined conformers were selected to represent the solution structure of the Cyp–CsA complex. For none of these conformers did the Lennard-Jones potential, torsion-angle potential, NOE distance constraint potential and dihedral-angle constraint potential individually exceed the value given by the average over all 37 conformers plus the standard deviation. This cutoff criterion correlated well with the residual DIANA target function: The final set of 22 conformers includes nine of the 10 DIANA conformers with lowest target functions, but only two out of the seven conformers that had been selected from the plateau with $rmsd_{max}$ = 1.87 Å (see Fig. 4).

A superposition for best fit of the polypeptide backbone atoms N, C^{α} and C' of the complete polypeptide chains of Cyp and CsA in the 22 conformers yields an average rmsd relative to the mean structure of 1.10 Å for the backbone atoms and 1.67 Å for all heavy atoms (Table 2). The corresponding values for the well-defined regions of Cyp identified in Table 2 and all residues of CsA are 0.68 and 1.24 Å, and similar rmsd values were obtained when only the regular secondary structures of Cyp and all residues of CsA were considered. The conformation of bound CsA alone is significantly better defined, with a backbone rmsd of 0.20 Å. If only the binding-site residues of Cyp and CsA are considered for the superposition, the backbone rmsd is 0.74 Å, indicating that the relative positioning of receptor and ligand is better defined than the structure of the entire complex. The precision of the structure determination varies significantly along the amino acid sequence: In addition to the chain-terminal residues, the peptide segments 40–55, 63–75 and 148–149 of Cyp show increased disorder (Figs. 5 and 6A). As an illustration of the quality of the determination of side-chain conformations in the structure of the complex, local superpositions of the peptide segments 119–126 (3_{10}-helix) of Cyp and of the bound CsA are shown in Fig. 7.

The solution structure of the Cyp–CsA complex

Inspection of the 3D Cyp–CsA structure starting from the N-terminus shows eight β-strands, which constitute an antiparallel β-barrel that dominates the molecular architecture of Cyp, with residues 4–11 (β-strand I), 16–24 (II), 55–56 (VII), 61–64 (VI), 96–101 (IV), 111–115 (V), 129–132 (III) and 155–164 (VIII). These β-strands coincide well with the β-sheet topology identified previously by an empirical pattern-recognition approach (Wüthrich et al., 1991b). Several well-defined β-turns are found near the surface of the protein at positions 12–15 (type I', connecting the strands I and II), 57–60 (type II, connecting strands III and IV), 77–80 (type I), 104–107 (type II) and 147–150 (type I). Local structures formed by residues 42–45 and 48–51 are characterized as tight turns by HN_{i+3}-O'_i hydrogen bonds, but they are not sufficiently well determined to be

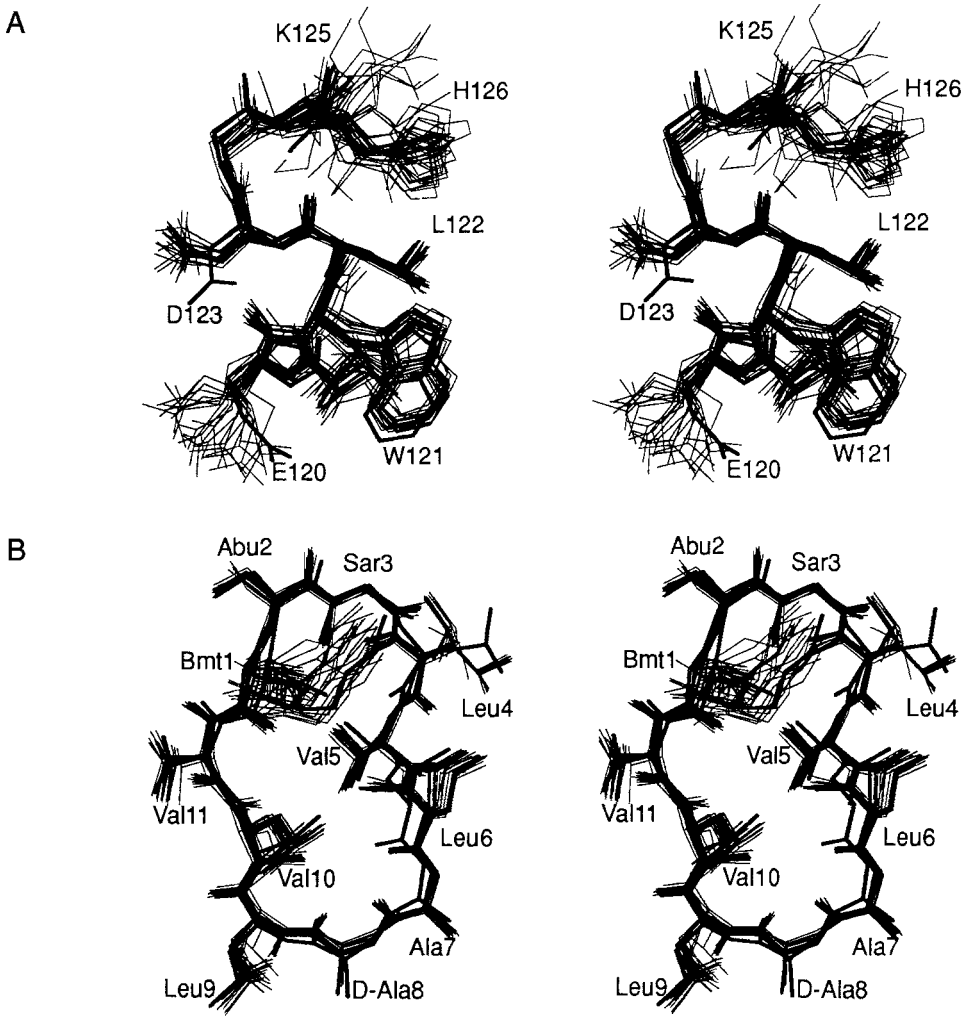

Fig. 7. Local superpositions of the 22 energy-minimized conformers of the solution structure (thin lines) of the Cyp–CsA complex with the crystal structure (thick line) for the following peptide segments: (A) Thr^{119}-His^{126} (TEWLDGKH); (B) CsA. The backbone atoms N, C^{α} and C' of the individual energy-refined DIANA conformers in the polypeptide segments shown were superimposed for minimal rmsd with the crystal structure of the complex (Pflügl et al., 1993).

attributed unambiguously to one of the common types of β-turns (e.g., Richardson, 1981). The β-sheet contains a number of β-bulges (Wüthrich et al., 1991b; Ke, 1992) which, with the exception of the two bulges at residues 17–18 and 159–160, occur primarily at the edges of the regular β-strands. For most of the β-bulges, bifurcated interstrand hydrogen bonds are observed, although the hydrogen bond between NH of residue 2 of the bulge and the acceptor was in most instances identified only in a small proportion of the 22 NMR conformers (the following hydrogen-bonding criteria were used: the proton–acceptor distance must be shorter than 2.4 Å, and the angle between donor–proton bond and the line connecting the donor and acceptor heavy atoms must be smaller than 35°). The following β-bulges were identified (we follow the notation by Richardson (1981), with residue 1-residue 2/acceptor residue): Leu^{17}-Gly^{18}/Ile^{10}; Phe^{60}-Met^{61}/Ile^{57};

Phe^{129}-Gly^{130}/Leu^{98}; Lys^{133}-Glu^{134}/Ser^{21}; Ala^{159}-Asp^{160}/Asp^{9}. A bifurcated hydrogen bond was also observed for Gly^{96}-Ile^{97}/Cys^{115}, where the well-defined backbone dihedral angles for the peptide segment Pro^{95}-Gly^{96}-Ile^{97} with $\psi_{95} = 148°$; $\varphi_{96} = 90°$; $\psi_{96} = 22°$; $\varphi_{97} = -108°$ and $\psi_{97} = 120°$ indicate that Gly^{96} and Ile^{97} form a G1-bulge. Simultaneously, Pro^{95} and Gly^{96} are i+2 and i+3 residues of a type II turn, although with the above criteria the hydrogen bond Ile^{97} NH-Gly^{94} O' is not identified either in the present NMR structure or in the crystal structure of Cyp (Ke, 1992). Residues 51–54 are not sufficiently well defined in the NMR structure to allow for an unambiguous assignment of the secondary structure type, although backbone–backbone hydrogen bonds identified in a small proportion of the conformers would agree with the previous assignment of this polypeptide segment in the crystal structure of Cyp (Ke, 1992) as a β-strand, followed by the β-bulge His^{54}-Arg^{55}/Gln^{63}.

Two helices cover the two open areas of the β-barrel (Fig. 6B). Helix 1 comprises residues 29–42, with a continuous succession of α-helix-type hydrogen bonds. It is preceded by a loop with the α-helix-type hydrogen bond Val^{29} NH-Phe^{25} O' which clearly does not represent an N-terminal elongation of the helix (Fig. 6B). Helix 2 has α-helix-type O'-HN hydrogen bonds in the polypeptide segment 135–143, and a 3_{10}-helix turn at residues 144–146. The presence of hydrogen bonds between NH of residue 144 and, with about equal probability in the 22 conformers, C' = O of the two residues 140 and 141 manifests directly the transition from the α-helical to the 3_{10}-helical part of helix 2. In the loop from the CsA binding-site residues 116–130, which includes the essential Trp^{121} residue, residues 119–123 have a 3_{10}-helical conformation characterized by O'-HN hydrogen bonds between residues 122–119 and 123–120, but otherwise no regular secondary structure could be identified.

The conformation of Cyp-bound CsA is well defined and closely related to the conformation that was previously determined by NMR in solution (Fesik et al., 1991; Weber et al., 1991), with one exception. The rather large rmsd of 0.72 Å relative to the previously proposed model (Table 2) is mainly due to changes of the side-chain orientation of MeBmt^{1}. Additional conformational constraints, based on the assignment of the side-chain γ-hydroxyl proton (see above), resulted in a well-defined side-chain conformation of MeBmt in the presently reported structure, with $\chi^1 = -43 \pm 15°$ and the hydroxyl group directed over the CsA ring to form a transannular hydrogen bond to the carbonyl oxygen of MeLeu^{4}.

In the regular secondary structure elements identified in CsA-bound Cyp, the expected hydrogen bonds are well defined in the NMR structure, and the structure also agrees well with the previously reported data on slowed exchange of backbone amide protons (Wüthrich et al., 1991b).

Intermolecular interactions between CsA and Cyp

A Y-shaped CsA binding pocket is formed by the four β-strands III, IV, V and VI (Fig. 6) and the loops of residues 65–75, 102–110, 117–128 and 147–150. The eight residues Phe^{60}, Ala^{101}, Asn^{102}, Ala^{103}, Phe^{113}, Trp^{121}, Leu^{122} and His^{126} of Cyp, and MeLeu^{9}, MeLeu^{10}, MeVal^{11}, MeBmt^{1} and Abu^{2} of CsA form intermolecular contacts with heavy-atom distances of less than 4.5 Å. These are consistently found in the 22 NMR conformers, with standard deviations of less than ± 0.5 Å (Table 3). In addition, the long side chains of residues Arg^{55}, Met^{61} and Gln^{111} are also located within the immediate binding site and show intermolecular NOEs to CsA protons, but their conformations are not sufficiently well defined to warrant a precise identification of the interatomic contacts.

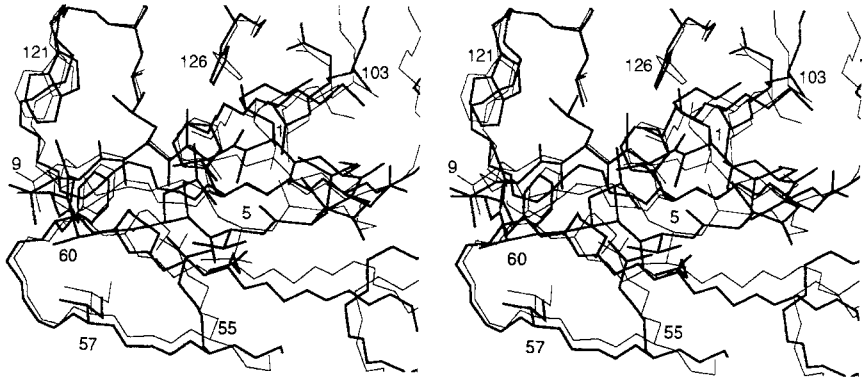

Fig. 8. Stereoview of the binding site in the NMR conformer with the lowest residual energy of the Cyp–CsA complex (thick line) and comparison to the crystal structure of Pflügl et al. (1993) (thin line). The backbone atoms N, C^{α} and C' of the binding-area residues as defined in footnote d of Table 2 have been superimposed for minimal rmsd. For the NMR conformer, all side chains of CsA and those of Cyp that belong to the ligand binding site are shown. For improved clarity, the solvent-exposed side chains of CsA have been omitted from the crystal structure.

A detailed view of the CsA binding site is afforded by Fig. 8: Tight hydrophobic interactions of the Cyp residues in a central cavity, i.e., Phe^{60}, Met^{61}, Ala^{101}, Phe^{113} and Leu^{122}, with the side chain of $MeVal^{11}$ from CsA are critical for the relative positioning of CsA and Cyp. As was previously shown (Spitzfaden et al., 1992a), the $MeVal^{11}$ side chain occupies the same location as

TABLE 3
SHORT INTERMOLECULAR CONTACTS BETWEEN Cyp AND CsA[a]

Cyp[b]	CsA[b]	Cyp[b]	CsA[b]
60 Phe C^{δ}	9 MeLeu C^{β}	103 Ala C^{α}	1 MeBmt C^{β}
60 Phe C^{ε}	9 MeLeu C^{α}, C^{β}, C', O'		2 Abu N
	11 MeVal $C^{\gamma 2}$	103 Ala C^{β}	2 Abu N, C^{α}, C^{β}, C', O'
60 Phe C^{ζ}	9 MeLeu C^{α}, C^{β}, C', O'	103 Ala O'	1 MeBmt C^{η}
	11 MeVal $C^{\gamma 2}$	113 Phe C^{β}, C^{γ}, C^{δ}	11 MeVal $C^{\gamma 1}$
101 Ala C^{α}	11 MeVal O'	121 Trp $C^{\delta 1}$	9 MeLeu O'
101 Ala C^{β}	1 MeBmt O'		10 MeLeu $C^{\delta 2}$
	2 Abu C^{γ}	121 Trp $C^{\varepsilon 2}$	9 MeLeu O'
	11 MeVal $C^{\gamma 1}$, O', C'	121 Trp $N^{\varepsilon 1}$	9 MeLeu NC, C', O'
101 Ala C'	11 MeVal O'		10 MeLeu $C^{\delta 2}$
102 Asn N	2 Abu C^{γ}	121 Trp $C^{\zeta 2}$	9 MeLeu C^{β}, O'
102 Asn N	11 MeVal O'	122 Leu C^{γ}	11 MeVal CN
102 Asn C^{α}	2 Abu C^{γ}	122 Leu $C^{\delta 1}$	11 MeVal CN, $C^{\gamma 2}$
102 Asn C'	1 MeBmt C^{α}, C^{β}, $C^{\delta 2}$	122 Leu $C^{\delta 2}$	11 MeVal CN
	2 Abu N, C^{γ}	126 His N^{δ}	11 MeVal CN, O'
102 Asn O'	1 MeBmt C^{β}, $C^{\gamma 1}$, $C^{\delta 2}$	126 His C^{ε}	1 MeBmt $C^{\delta 2}$
	11 MeVal O'		11 MeVal CN, C', O'
103 Ala N	2 Abu N, C^{γ}	126 His N^{ε}	1 MeBmt $C^{\delta 2}$

[a] Contacts are listed if the average of the intermolecular distances between distinct heavy atoms in the final 22 energy-minimized NMR conformers is shorter than 4.5 Å, and the standard deviation is less than 0.5 Å.

[b] The interacting atoms are identified by residue number, amino acid type and atom position. Atoms of Cyp with multiple intermolecular contacts are listed only once.

the prolyl residue of substrates for *cis-trans* isomerase activity of Cyp. Furthermore, CsA is quite tightly fixed by interactions of the side chains of MeBmt[1] and Abu[2], which contact the peptide segment 101–103 of Cyp from both sides. At the opposite end of the molecule, the side chain of MeLeu[9] interacts with Trp[121] and Phe[60] of Cyp. That these interactions in the central cavity have functional significance is implicated by site-directed mutagenesis of Phe[60] and Phe[113] of Cyp (Zydowsky et al., 1992), as well as by chemical modification of the CsA segment MeVal[11] to Abu[2] (Wenger, 1986), which both strongly affect CsA binding.

The hydrophobic cavity that accommodates the side chain of MeVal[11] in the Cyp–CsA complex is surrounded by the uncharged, or positively charged, hydrophilic residues His[54], Arg[55], Gln[63], Thr[73], Asn[102], Gln[111], Trp[121] and His[126]. Of these, Arg[55], Gln[63], Asn[102], Trp[121] and His[126] form specific intermolecular hydrogen bonds with CsA. Of particular interest with regard to the interactions in enzymatically active Cyp complexes with substrates for *cis-trans* isomerase activity is the network of hydrogen bonds involving residues Arg[55], Asn[102] and His[126] of Cyp and the dipeptide segment MeLeu[10]–MeVal[11] of CsA. For example, in the present Cyp–CsA structure there is evidence that the guanidinium group of Arg[55] and MeVal[10] O' form a hydrogen bond. Corresponding hydrogen bonds were found between Arg[55] and the prolyl carbonyl group in the crystal structures of Cyp in complexes with linear peptide substrates (Kallen and Walkinshaw, 1992; Ke et al., 1993). The carbonyl oxygen of MeVal[11] can form hydrogen bonds either to the backbone amide proton of Asn[102] or to $N^{\varepsilon}H$ of His[126]. In the case of His[126], closer approach than 3.0 Å with the $N^{\varepsilon}H$ and $C^{\varepsilon}H$ protons is observed in 11 and 18 of the 22 NMR conformers, respectively, indicating the presence of a geometrically distorted hydrogen bond.

Comparison with other structure determinations of the Cyp–CsA complex

Visual comparisons of the presently determined Cyp–CsA structure with the results of the structure determinations mentioned in the Introduction showed close similarity between all these structures, including in particular also the NMR solution structure reported by Thériault et al. (1993). However, atomic coordinates as a basis for quantitative comparisons are currently available only for the crystal structure of Pflügl et al. (1993) and the molecular model proposed by Spitzfaden et al. (1992a) from a combination of crystallographic and NMR data. The rmsd values for these two structures are 0.6 Å for the backbone atoms N, C^{α} and C', and 1.2 Å for all heavy atoms. The global rmsd values for different atom selections (Table 2) are nearly identical for the crystal structure and the molecular model, with the sole exception of those for CsA (see below). The plots of displacements and local rmsd values in Fig. 5 further show that the differences between the solution structure and either the crystal structure or the molecular model correlate closely with the global displacements of the solution structure itself (Fig. 5A). The rmsd values obtained after local superposition of consecutive tripeptide segments (Fig. 5B) show that the three structures are locally very similar, even in the poorly defined loop regions 65–75 and 147–150. A notable difference to this generally close fit is observed for the turn of residues 12–15 (Fig. 5B), which is a type I-turn in the crystal structure of the Cyp–CsA complex (Pflügl et al., 1993) and a reverse type I-turn in the presently determined NMR structure. Close coincidence between the NMR and X-ray structures is also seen in Fig. 8 for the intermolecular contact region. As illustrated by Fig. 7, the crystal structure is, with the exception of only a few residues, contained within the conformational space sampled by the 22 NMR conformers, which shows in a very direct way that few significant structural differences can be identified.

An important local difference between the molecular model of Spitzfaden et al. (1992a) on the one hand and the complete structure determinations for the complex either by X-ray diffraction or by NMR (Pflügl et al., 1993; Thériault et al., 1993; this paper) on the other hand was identified for the side chain of MeBmt[1] of CsA. The origin of this structural difference can be traced back to the fact that the MeBmt[1] side chain was only poorly defined in the initial structure of Cyp-bound CsA (Weber et al., 1991). For the building of the complex there was extensive freedom in choosing the orientation of the hydroxyl group of MeBmt[1], and an intermolecular hydrogen bond with the carbonyl oxygen of Asn[102] of Cyp was energetically most favorable. The additional NOE constraints collected now on the basis of the assignment of the MeBmt[1] hydroxyl proton resonance are incompatible with this intermolecular hydrogen bond; instead, these constraints define an intramolecular hydrogen bond to the carbonyl oxygen of MeLeu[4] of CsA. The same local structure was found in the crystal structure (Pflügl et al., 1993) and the NMR structure by Thériault et al. (1993).

ACKNOWLEDGEMENTS

We would like to thank Dr. K. Memmert for help with the fermentation and cyclophilin A production, Dr. B. Messerle and Dr. J. Moore for participation in the early stages of the resonance assignments, Ch. Bartels for support in the use of the programs EASY and XEASY, and Mrs. E. Huber for the careful processing of the manuscript. The use of the Cray Y-MP of the ETH Zürich and financial support by the Schweizerischer Nationalfonds (Project 31.32033.91) are gratefully acknowledged.

REFERENCES

Bax, A., Clore, G.M. and Gronenborn, A.M. (1990) *J. Magn. Reson.*, **88**, 425–431.
Billeter, M., Kline, A.D., Braun, W., Huber, R. and Wüthrich, K. (1989) *J. Mol. Biol.*, **206**, 677–687.
Borel, J.F. (Ed.) (1986) *Ciclosporin*, Karger, Basel.
Braun, W. and Gō, N. (1985) *J. Mol. Biol.*, **186**, 611–626.
Braun, W. (1987) *Q. Rev. Biophys.*, **19**, 115–157.
Clore, G.M., Kay, L.E., Bax, A. and Gronenborn, A.M. (1991) *Biochemistry*, **30**, 12–18.
Eccles, C., Güntert, P., Billeter, M. and Wüthrich, K. (1991) *J. Biomol NMR*, **1**, 111–130.
Ferrin, T.E., Conrad, C.H., Laurie, E.J. and Langridge, R. (1988) *J. Mol. Graphics*, **6**, 13–27.
Fesik, S.W. and Zuiderweg, E.R.P. (1988) *J. Magn. Reson.*, **78**, 588–593.
Fesik, S.W., Eaton, H.L., Olejniczak, E.T., Zuiderweg, E.R.P., McIntosh, L.P. and Dahlquist, F.W. (1990) *J. Am. Chem. Soc.*, **112**, 886–888.
Fesik, S.W., Gampe, R.T., Eaton, H.L., Gemmecker, G., Olejniczak, E.T., Neri, P., Egan, D.A., Edalji, R., Simmer, R., Helfrich, R., Hochlowski, J. and Jackson, M. (1991) *Biochemistry*, **30**, 6574–6583.
Fesik, S.W., Neri, P., Meadows, R., Olejniczak, E.T. and Gemmecker, G. (1992) *J. Am. Chem. Soc.*, **114**, 3165–3166.
Fischer, G., Wittmann-Liebold, B., Lang, K., Kiefhaber, T. and Schmid, F.X. (1989) *Nature*, **337**, 476–478.
Güntert, P. and Wüthrich, K. (1991) *J. Biomol. NMR*, **1**, 447–456.
Güntert, P., Braun, W. and Wüthrich, K. (1991a) *J. Mol. Biol.*, **217**, 517–530.
Güntert, P., Qian, Y.Q., Otting, G., Müller, M., Gehring, W.J. and Wüthrich, K. (1991b) *J Mol. Biol.*, **217**, 531–540.
Güntert, P., Dötsch, V., Wider, G. and Wüthrich, K. (1992) *J. Biomol. NMR*, **2**, 619–629.
Haendler, B., Hofer-Warbrinek, R. and Hofer, E. (1987) *EMBO J.*, **6**, 947–950.
Handschuhmacher, R.E., Harding, M.W., Rice, J., Drugge, R.J. and Speicher, D.W. (1984) *Science*, **226**, 545–547.
Ikura, M., Kay, L.E., Tschudin, R. and Bax, A. (1990) *J. Magn. Reson.*, **86**, 204–209.
Kallen, J., Spitzfaden, C., Zurini, M.G.M., Wider, G., Widmer, H., Wüthrich, K. and Walkinshaw, M.D. (1991) *Nature*, **353**, 276–279.

Kallen, J. and Walkinshaw, M.D. (1992) *FEBS Lett.*, **300**, 286–290.
Ke, H. (1992) *J. Mol. Biol.*, **228**, 539–550.
Ke, H., Mayrose, D. and Cao, W. (1993) *Proc. Natl. Acad. Sci. USA*, **90**, 3324–3328.
Kraulis, P. (1991) *J. Appl. Crystallogr.*, **24**, 946–950.
Loosli, H.R., Kessler, H., Oschkinat, H., Weber, H.P., Petcher, T.J. and Widmer, A. (1985) *Helv. Chim. Acta*, **66**, 682–703.
Marion, D., Kay, L.E., Sparks, S.W., Torchia, D.A. and Bax, A. (1989) *J. Am. Chem. Soc.*, **111**, 1515–1517.
Messerle, B.A., Wider, G., Otting, G., Weber, C. and Wüthrich, K. (1989) *J. Magn. Reson.*, **85**, 608–613.
Michnick, S.W., Rosen, M.K., Wandless, T.J., Karplus, M. and Schreiber, S.L. (1991) *Science*, **252**, 836–839.
Moore, J.M., Peattie, D.A., Fitzgibbon, M.J. and Thomson, J.A. (1991) *Nature*, **351**, 248–250.
Némethy, G., Pottle, M.S. and Scheraga, H.A. (1983) *J. Phys. Chem.*, **87**, 1883–1887.
Neri, D., Szyperski, T., Otting, G., Senn, H. and Wüthrich, K. (1989) *Biochemistry*, **28**, 7510–7516.
Neri, P., Meadows, R., Gemmecker, G., Olejniczak, E., Nettesheim, D., Logan, T., Simmer, R., Helfrich, R., Holzman, T., Severin, J. and Fesik, S. (1991) *FEBS Lett.*, **294**, 81–88.
Otting, G. and Wüthrich, K. (1990) *Q. Rev. Biophys.*, **23**, 39–96.
Pflügl, G., Kallen, J., Schirmer, T., Jansonius, J.N., Zurini, M.G.M. and Walkinshaw, M.D. (1993) *Nature*, **361**, 91–94.
Powers, R., Gronenborn, A.M., Clore, G.M. and Bax, A. (1991) *J. Magn. Reson* , **94**, 209–213.
Richardson, J.S. (1981) *Adv. Protein Chem.*, **23**, 283–437.
Sanner, M., Widmer, A., Senn, H. and Braun, W. (1989) *J. Comput.-Aided Mol. Design*, **3**, 195–210.
Schaumann, T., Braun, W. and Wüthrich, K. (1991) *Biopolymers*, **29**, 679–694.
Schreiber, S.L. (1991) *Science*, **251**, 283–287.
Spitzfaden, C., Weber, H.P., Braun, W., Kallen, J., Wider, G., Widmer, H., Walkinshaw, M.D. and Wüthrich, K. (1992a) *FEBS Lett.*, **300**, 291–300.
Spitzfaden, C., Bartels, C., Wider, G., Braun, W., Widmer, H. and Wüthrich, K. (1992b) *NMR Structure Determination of the Cyclophilin–Cyclosporin Complex*, XV International Conference on Magnetic Resonance in Biological Systems, Jerusalem.
Takahashi, N., Hayano, T. and Suzuki, M. (1989) *Nature*, **337**, 473–475.
Thériault, Y., Logan, T.M., Meadows, R., Yu, L., Olejniczak, E.T., Holzman, T.F., Simmer, R.L. and Fesik, S.W. (1993) *Nature*, **361**, 88–91.
Van de Ven, F.J.M. and Philippens, M.E.P. (1992) *J. Magn. Reson.*, **97**, 637–644.
Von Freyberg, B. and Braun, W. (1993) *J. Comput. Chem.*, **14**, 510–521.
Von Freyberg, B., Schaumann, T. and Braun, W. (1993a) *FANTOM*, V3.1, User Manual, ETH, Zürich.
Von Freyberg, B., Richmond, T.J. and Braun, W. (1993b) *J. Mol. Biol.*, **233**, 275–292.
Weber, C., Wider, G., Von Freyberg, B., Traber, R., Braun, W., Widmer, H. and Wüthrich, K. (1991) *Biochemistry*, **30**, 6563–6574.
Wenger, R.M. (1986) In *Ciclosporin* (Ed, Borel, J.F.) Karger, Basel, pp. 28–45.
Wider, G., Weber, C., Traber, R., Widmer, H. and Wüthrich, K. (1990) *J. Am. Chem. Soc.*, **112**, 9015–9016.
Wider, G., Weber, C. and Wüthrich, K. (1991) *J. Am. Chem. Soc.*, **113**, 4676–4678.
Widmer, H., Widmer, A. and Braun, W. (1993) *J. Biomol. NMR*, **3**, 307–324.
Williamson, M.P., Havel, T.E. and Wüthrich, K. (1985) *J. Mol. Biol.*, **182**, 295–315.
Wüthrich, K., Billeter, M. and Braun, W. (1983) *J. Mol. Biol.*, **169**, 949–961.
Wüthrich, K. (1986) *NMR of Proteins and Nucleic Acids*, Wiley, New York, NY.
Wüthrich, K., Von Freyberg, B., Weber, C., Wider, G., Traber, R., Widmer, H. and Braun, W. (1991a) *Science*, **254**, 953–954.
Wüthrich, K., Spitzfaden, C., Memmert, K., Widmer, H. and Wider, G. (1991b) *FEBS Lett.*, **285**, 237–247.
Xia, T.H. (1992) Ph.D. Thesis, ETH, Zürich.
Zuiderweg, E.R.P., McIntosh, L.P., Dahlquist, F.W. and Fesik, S.W. (1990) *J. Magn. Reson.*, **86**, 210–216.
Zuiderweg, E.R.P., Petros, A.M., Fesik, S.W. and Olejniczak, E.T. (1991) *J. Am. Chem. Soc.*, **113**, 370–372.
Zydowsky, L.D., Etzkorn, F.A., Chang, H.Y., Ferguson, S.B., Stolz, L.A., Ho, S.I. and Walsh, C. (1992) *Protein Sci.*, **1**, 1092–1099.